Ultrafast Dissociation Dynamics of Ferrocene and [3]-Ferrocenophan[†]

M. Clara and H. J. Neusser*

Institut für Physikalische und Theoretische Chemie, Technische Universität München, Lichtenbergstrasse 4, D-85748 Garching, Germany

Received: July 27, 2000; In Final Form: December 6, 2000

We present pump−probe results for ferrocene and [3]-ferrocenophan measured with two 200-fs UV laser pulses of different wavelengths. The molecules are excited by single-photon absorption to a fast decaying intermediate state and ionized by absorption of a second photon. The so-produced parent cations can absorb further photons until their internal energy is sufficient to open different fragmentation channels. Because of the broad absorption spectra of ferrocene, each laser pulse can act as a pump and probe pulse. We use the rotating wave approximation of the Schrödinger equation of a three-level system to numerically calculate the population dynamics of the neutral excited state, the parent ion, and the fragment ions produced after absorption of further photons in the ferrocene cation. From the observed transients in the ferrocene cation signal, a dissociation time of 200 fs of the neutral excited ferrocene is found and the same dissociation time is measured for [3]-ferrocenophan, where the rings are bridged. This points to a concerted, multiple metal−ligand bond break after photon absorption, which is not hindered by the bridge. From a comparison of measured and calculated transients in the fragment ion signal, we conclude that the observed fragment ions originate from a dissociation of the ferrocene cation rather than from a neutral dissociation and subsequent ionization.

I. Introduction

Ultrashort laser pulses combined with molecular beam techniques and time-of-flight (TOF) mass spectroscopy represent an important tool for investigating the dynamics of molecular systems.[1] Organometallic compounds are known to undergo a fast dissociation process after electronic excitation. The dissociation dynamics of the cyclopentadienyliron dicarbonyl dimer $[CpFe(CO)_2]_2$ was measured in a real-time experiment by Berget et al.[2] on a femtosecond time scale. The multiple bond breaking time of the metal−CO, the metal−metal, and the metal−Cp bond varies between 35 and 900 fs. The fragmentation pattern of another organometallic compound, the monometal carbonyl $Fe(CO)_5$, depends strongly on the laser wavelength, the laser intensity, and the laser pulse duration.[3] The fs pump−probe transient points to a breaking of the metal−CO bonds within 100 fs. In a comparable experiment with $Mn_2(CO)_{10}$, the two different bond types, namely, the metal−metal and metal−ligand bonds, lead to different cleavage dynamics.[4]

Little is known about the ultrafast dissociation dynamics of another prototype organometallic sandwich compound, Ferrocene (see Figure 1a). Its chemical and photophysical properties have been investigated by various groups (refs 5 and 6 and references therein). Studying its dissociation pathways leads to a better understanding of the involved charge-transfer process, playing a central role in excited-state chemistry. Gaseous ferrocene has more or less structureless absorption bands with broad peaks[7] in the interesting wavelength range from 272 to 237 nm. Therefore from the absorption spectra precise information about the quantum chemical properties and the dynamic processes of the molecule, e.g., vibrational frequencies or moments of inertia, cannot be obtained. It also absorbs in the visible, leading to the yellow color. One reason for the broad
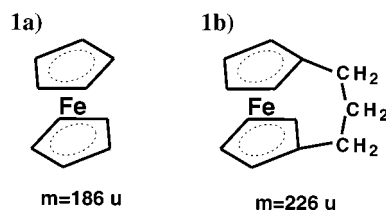
Figure 1. Ferrocene derivatives investigated in this work: (a) Ferrocene. (b) [3]-Ferrocenophan.

spectra is the large number of vibrational modes (57 internal degrees of freedom) and a high density of electronic states of various multiplicities. Some of the smooth features in the absorption spectrum were assigned to d−d transitions in Fe, metal-to-ligand or ligand-to-metal charge-transfer transitions, and electronic transitions within the cyclopentadienyl (Cp) rings.[7]

In a series of multiphoton dissociation (MPD)/multiphoton ionization (MPI) studies of ferrocene[8−15] with nanosecond (ns) laser pulses at various wavelengths in the near-UV and the visible (UV/VIS), it has been shown that one or both Cp ligands are lost prior to ionization when a resonant intermediate state is excited in the multiphoton process. As a consequence, no intact ferrocene cations were observed in the mass spectra. The central Fe atom loses its Cp rings after absorption of one or more UV photons (neutral channel), and the uncharged Fe atom can be ionized and thus detected by resonance-enhanced multiphoton ionization when the laser wavelength is close to an atomic resonance. The detailed mechanism of photon absorption, energy redistribution and dissociation has not been unequivocally established. It was concluded that the dynamics of the dissociation process depends on the chosen photon energy as well as on the laser fluence. Two competing dissociation mechanisms, one via statistical redistribution,[11] the other via direct dissociation,[12,13] are thought to be possible.

From thermochemical studies[16−18] the dissociation energy for the decomposition of ferrocene into a neutral Fe atom and two Cp radicals is found to be 6.2 eV. Elimination of only one Cp ring requires an energy of 4 eV,[16] which is noticeably more than necessary for removing the remaining second Cp ring.

While resonance-enhanced multiphoton ionization with typical photon energies $h\nu \leq 6.2$ eV failed to produce parent ions, one-photon vacuum ultraviolet (VUV) ionization of ferrocene has led to intact ferrocene ions.[19−21] Determination of the ionization energy (IE) of ferrocene by one-photon VUV or electron impact ionization yielded slightly differing values in the range between 6.61 and 7.15 eV.[15,20−33] With increasing photon energy new dissociation channels are opened.[19−21] E.g., the appearance energy for the ferrocene fragment $Fe(Cp)^+$ lies between 11.6 and 14.38 eV. In this energy range three other fragments of the ferrocene cation appear: The Fe^+, $Fe(Cp)C_3H_3^+$, and $(Cp)_2^+$ ion.

Recently, we were able to show that multiphoton ionization with *femtosecond* pulses can compete with the fast dissociation process in the intermediate states of ferrocene, leading to the appearance of parent ions[34] and fragment ions. In particular, we found another channel for the production of Fe^+, i.e., the ionic channel, which is also active in VUV and electron impact mass spectrometry. As the fragmentation pattern was found to be identical with that of VUV experiments leading to a comparable internal energy, this can be taken as an indication of a statistical behavior in ion fragmentation. Grotemeyer and co-workers reported, that it was possible to produce ferrocene ions with UV femtosecond laser pulses with a laser pulse duration of 500 fs.[35] A simultaneous fragmentation of the parent ion was not observed, in contrast to $Fe(CO)_5$.[35,36]

In this work we present the, to our best knowledge, first time-resolved results for the dynamics of the dissociation process of ferrocenes. The dynamic behavior is investigated in a pump−probe experiment at different photon energies. The excited electronic transitions are assigned to metal-to-ligand, ligand-to-metal charge-transfer transitions and to transitions within the Cp rings.[7] For an understanding of the time behavior, it is important to discuss the different neutral dissociation and ionic fragmentation channels. The experimentally found transients at several masses are interpreted by a dynamic model within the rotating wave approximation. In ferrocene a special situation exists, which differs from the previously published pump−probe experiments, where only the pump pulse causes a dissociation. Because of the broad absorption bands of ferrocene spanning a wavelength range from 550 to 185 nm, each of the laser pulses can act as pump− and as probe−pulse at the same time. This is taken into account in the dynamic model presented in this work. In this way the typical dissociation time for the electronically excited ferrocene molecules is deduced. Furthermore the influence of a bridge between the two Cp rings ([3]-ferrocenophan, Figure 1b) on the photochemical stability is investigated and compared with that of the unbridged ferrocene.

II. Experimental Section

The experimental set up is described in detail elsewhere.[37] A schematic drawing of the femtosecond set up is shown in Figure 2. Briefly, cold ferrocene molecules in a supersonic molecular beam are produced by expansion of ferrocene vapor through a heated CW nozzle (orifice: 300 μm ϕ) into a vacuum chamber. The typical temperature of the nozzle is 120 °C. After passing a skimmer with an entrance aperture of 3 mm ϕ, the molecules interact with the femtosecond laser pulses of a slightly focused laser beam. The interaction zone of the laser beam and
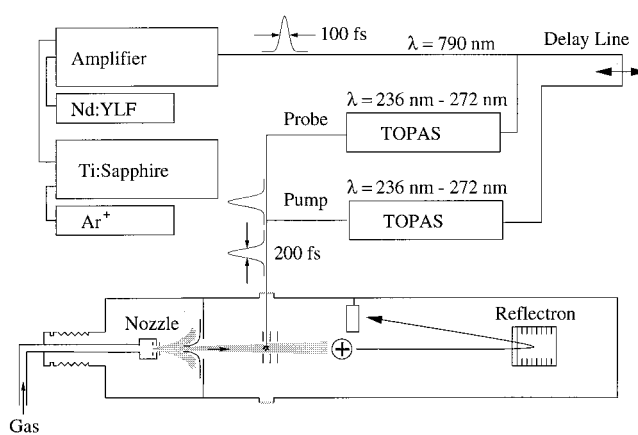

Figure 2. Scheme of the experimental set up for the femtosecond pump−probe experiment in a skimmed cold molecular beam with mass analysis in a reflecting time-of-flight mass spectrometer. The amplified femtosecond light pulses are frequency converted in a TOPAS system leading to UV pump and probe pulses of different wavelengths and 200 fs (fwhm) duration. For details, see text.

the molecules is placed in the center of the ion optics of a reflecting time-of-flight mass spectrometer.[38] Here the ferrocene molecules are excited and ionized by a UV femtosecond pulse with a variable wavelength between 272 and 236 nm. The mass spectra of ferrocene and [3]-ferrocenophan were recorded with a laser pulse energy of 40 μJ and a peak intensity of about 2 x 10^{12} W cm^{-2}. The pulse energy was decreased to 1 μJ in the pump−probe experiments, yielding a peak intensity of about 5 x 10^{10} W cm^{-2} to avoid saturation effects. We carefully adjusted the two laser beams to achieve an optimum two-color signal by complete overlap of the laser foci.

The produced ions are accelerated in a repeller electronic potential of 1200 V toward the ion reflector and hit the multichannel plates after reflection. All mass spectra were recorded with a multichannel scaler/averager (Stanford Research Systems SR 430). The different pump−probe transients were recorded simultaneously after selection of the interesting masses with three gated integrators (Stanford Research Systems SR 250) and were processed in a microcomputer system.

The laser system consists of a commercial Nd:YLF amplifier (Super-Spitfire, Spectra Physics) seeded with an Ar^+ laser-pumped Ti:sapphire laser (Mira Basic, Coherent). The duration of the oscillator pulses at $\lambda = 790$ nm is 80 fs (fwhm) and of the amplified pulses 100 fs (fwhm). The pulse widths are monitored with a home-built interferometric autocorrelator with nonlinear photodiode detection.[39] The amplified light beam is directed into a traveling-wave optical parametric amplifier of superfluorescence (TOPAS, Light Conversion), where it pumps parametric processes. The Fourier transform limit is 200 fs for the UV pulses, which is about twice the value of the visible pulses, but the broadening can be explained by the length of the doubling crystal used in the experiment.

For the exact determination of the pulse lengths of the UV femtosecond pulses we measured the pump−probe signal for a nonresonant excitation of gas-phase benzene with a pump pulse photon energy of 37300 cm^{-1}, which is smaller than the pure electronic transition energy to the $S_1 \leftarrow S_0$ vibrational ground state at 38 086 cm^{-1}. The photon energy of the second probe pulse was fixed to the same value of 37 300 cm^{-1}, which is sufficient to reach the ionization energy (IE) in a two-photon two-color excitation experiment via a virtual intermediate state. In Figure 3 the measured ion current is plotted as a function of the delay of the probe pulse on a femtosecond scale. The resulting peak represents the crosscorrelation of the pump and

Dissociation Dynamics of Ferrocene

J. Phys. Chem. A, Vol. 105, No. 23, 2001 **5579**
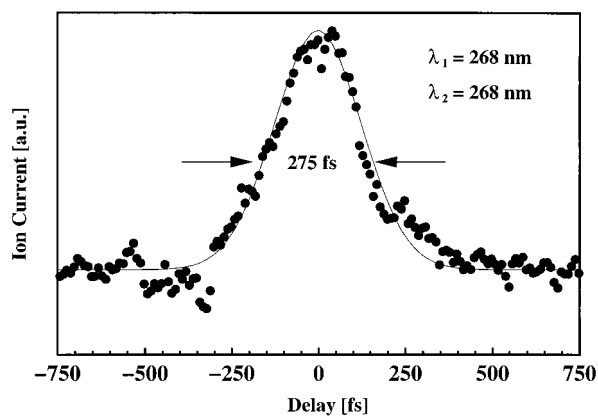
Figure 3. Crosscorrelation of two different UV femtosecond laser pulses with the same wavelength of 268 nm measured in a nonresonant pump−probe ionization process of benzene. The measured width of 275 fs of the crosscorrelation corresponds to a pulse length of 200 fs (fwhm) for the second-order autocorrelation of a Gaussian pulse.

Figure 4. Multiphoton mass spectrum of ferrocene recorded with femtosecond laser pulses at 244 nm. In the inset the intensity scale is magnified by a factor of 20.

Figure 5. Multiphoton mass spectrum of [3]-ferrocenophan recorded with 200 fs laser pulses at 244 nm. In the upper spectrum the intensity scale is magnified by a factor of 10.

probe pulse, since no real intermediate state is involved in the two-photon excitation process. The intensity ratio of the peak maximum to the baseline is close to the value of 3:1 expected for the maximum value of a crosscorrelation in a two-photon process. We find a width of 275 fs (fwhm) corresponding to a pulse width of 200 fs (fwhm) for the 2nd order autocorrelation of a Gaussian pulse.

[3]-Ferrocenophan was synthesized as described in ref 40.

III. Experimental Results

To investigate the dissociation behavior of ferrocene in metal-to-ligand or ligand-to-metal charge-transfer transitions between 30 800 and 37 700 cm^{-1} and an electronic transition located within the Cp ring at higher excitation energies,[7] we used different wavelengths between 237 and 272 nm for pump and probe pulses. The pulses at the fundamental wavelength of the TOPAS (472−544 nm) could be also used for ionization of excited-state ferrocene, but in ferrocene the visible probe laser wavelength would be in resonance with the d−d transition of the Fe in ferrocene.[7] As a consequence in this case a resonance-enhanced multiphoton absorption of the visible light pulse in the neutral ferrocene could not be excluded and the dynamics in the state with Fe character would complicate the interpretation of the measured transients. Furthermore, there is no clear preparation of final states in this case, since the total number of absorbed photons is not defined. For these reasons, we decided to perform the pump−probe experiment in ferrocene and [3]-ferrocenophan with two UV laser pulses of different wavelength in resonance with charge-transfer transitions to reduce the order of the multiphoton process.

A. Mass Spectra. *1. Mass Spectra of Ferrocene.* Resonance-enhanced two-photon ionization with nanosecond laser pulses ($h\nu \leq 6.2$ eV) leads to a strong Fe^+ peak,[8−15,34,41] but no parent (ferrocene) signal can be found. Neutral Fe is produced by a fast dissociation process before the absorption of a second photon results in the ionization of ferrocene. The so-produced neutral Fe is ionized very efficiently if the laser frequency is in resonance with an atomic transition of Fe, leading to the strong Fe^+ signal in the mass spectra. As we have shown in our recent work the result found for femtosecond laser pulses is quite different:[34] Here the intact ferrocene cation is the main feature in the mass spectra and many other molecular fragments larger than Fe^+ appear. Figure 4 shows a typical mass spectrum recorded in a one-laser experiment at 244 nm with the strongest
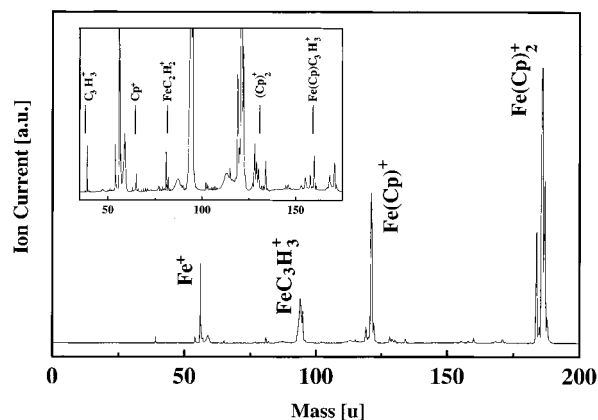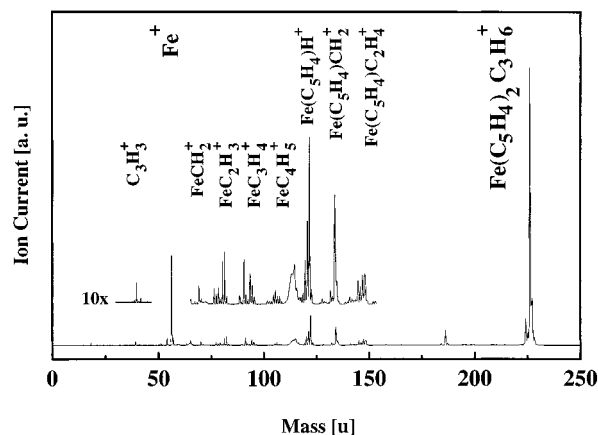
mass peak at 186 u originating from the parent ion and displaying the typical isotopic mass pattern of ferrocene. Three additional strong mass peaks are detected at 56, 95, and 121 u. The peaks at 121 and 95 u are assigned to $Fe(Cp)^+$ and $FeC_3H_3^+$, respectively. In addition Fe^+ (56 u) ions lead to a relatively strong signal. The other smaller peaks at 160, 130, 82, 65, and 39 u are assigned to $Fe(Cp)C_3H_3^+$, $(Cp)_2^+$, $FeC_2H_2^+$, Cp^+, and $C_3H_3^+$, respectively. From the intensity behavior of the different mass peaks and a comparison with the mass pattern of VUV measurements, we concluded that all fragment ion peaks originate from a fragmentation of the ferrocene parent ion.[34] This is similar to the case of $Fe(CO)_5$ for high laser intensities.[3] The production of neutral Fe occurring from the fast dissociation of ferrocene in the neutral intermediate state seems to be of minor importance, but cannot be excluded.

2. Comparison with Mass Spectra of Bridged Ferrocene. In further experiments we investigated the influence of a bridge between the two Cp rings on the photochemical stability.[34] From the similarity of the nanosecond mass spectra of the bridged [3]-ferrocenophan and ferrocene with a strong Fe^+ peak, we concluded that there is no stabilization by the bridge in the intermediate neutral excited state. After femtosecond excitation [3]-ferrocenophan can be ionized, leading to intact parent ions and a relatively strong Fe^+ ion peak but not to $FeCp^+$ as in the case of ferrocene (Figure 5).

This behavior points to a higher appearance energy of the respective channels in the bridged ferrocene. To open the lowest fragmentation channels of the [3]-ferrocenophan requires a
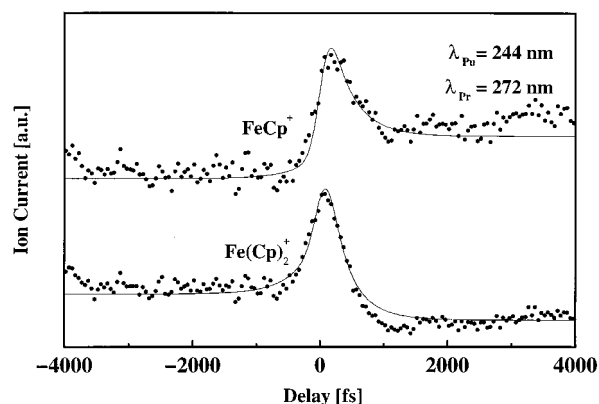
Figure 6. Ion current at the mass of ferrocene (lower trace) and the fragment FeCp$^+$ (upper trace) as a function of the delay time between pump pulse ($\lambda_{pu} = 244$ nm) and probe pulse ($\lambda_{pr} = 272$ nm). The height of the transient peaks is typically 30% of the maximum signal. The two traces have different zero levels and vertical scales (see different mass peak heights in Figure 4). The solid line represents the theoretical curve fitted to the measured transients (for details, see text). Positive delay corresponds to a delayed probe pulse, negative time means that the order of the pulses is inverted. Note, that in our experiment the absorption of photons from both laser pulses is possible by ground-state ferrocene.

higher energy than in the case of ferrocene, which is caused by the bridging of the two Cp rings. In addition to the bond breaking between the Fe and a Cp ring, which takes more than 4 eV, the necessary breaking of the C$-$C bond in the bridge requires about 3.6 eV. No special fragment seems to be preferred energetically.

B. Dynamics. *1. Ferrocene Cation and Its Main Fragment.* First, the dynamics in the intermediate state was recorded for pump pulses (λ_{pu}) at 244 nm (40 983 cm^{-1}) and delayed probe pulses (λ_{pr}) at 272 nm (36 765 cm^{-1}) (positive delay times). For negative delay times the pulses at 272 nm act as pump pulses and the pulses at 244 nm are the probe pulses. As described above this results from the broad absorption spectrum of ferrocene. To avoid confusion throughout the text we call the pulses acting as pump pulses for positive delay times as pump pulses even if they arrive later than the probe pulses for negative delay times. The excitation energy of 40 983 cm^{-1} leads to an electronic transition within a Cp ring. Photon energies lower than 37 700 cm^{-1} are expected to induce metal-to-ligand or ligand-to-metal charge-transfer transitions.

In Figure 6 the ion signals of the ferrocene cation (Fe(Cp)$_2$$^+$) at 186 u and the strongest fragmentation feature in the mass spectrum (Fe(Cp)$^+$) at 121 u as a function of the delay between the pump and probe pulses are shown. Both signals are detected simultaneously. The laser pulses at 244 nm are fixed at zero delay time. For longer delay times ($>+1$ ps, <-1 ps) a constant signal is observed. The constant ferrocene ion signal level is larger for negative delay times than for positive delay times. The fragment Fe(Cp)$^+$ shows the opposite behavior. The constant background level is smaller for negative delay times than for positive delay times. For delay times shorter than ±1 ps the transients in the ion signal show a subpicosecond dynamics which is different for Fe(Cp)$_2$$^+$ and Fe(Cp)$^+$. There is an increasing parent ion signal at -400 fs which decreases very rapidly for positive delay times. The half-width of this transient peak is about 530 fs, which is 1.9 times the width of the measured autocorrelation peak of the used laser pulses (see Figure 3). The simultaneous recorded fragment ion signal at 121 u (Fe(Cp)$^+$) shows a similar behavior. Here the peak width is in the same range, but an important difference is seen: The
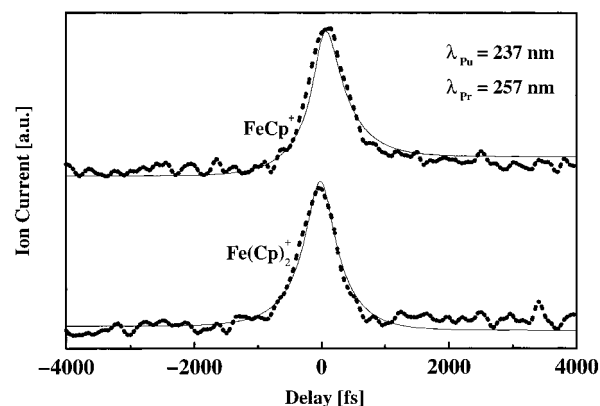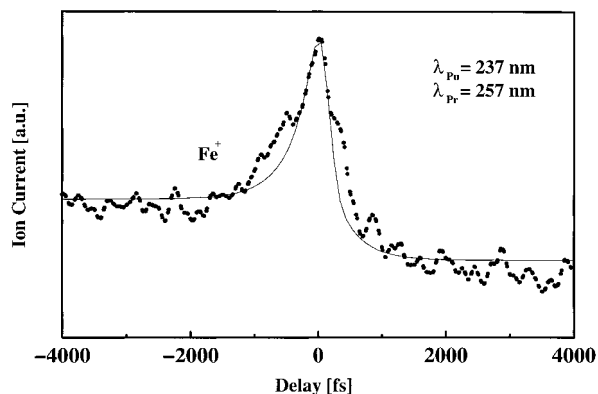

Figure 7. Two color subpicosecond transients measured at the mass of the ferrocene cation (lower trace) and the ferrocene fragment ion FeCp$^+$ (upper trace) for a pump pulse wavelength of 237 nm and a probe pulse wavelength of 257 nm. The two traces have different zero levels and vertical scales (see peak heights in Figure 4). The solid lines represent the best fit of the calculation (for details, see text).

maximum of the FeCp$^+$ signal is delayed by some 100 fs. This indicates that FeCp$^+$ results from a fragmentation of the ferrocene cation because the ferrocene cation has to be produced first before a dissociation can occur, this leading to the observed delay. For a two-color pump$-$probe experiment where both laser pulses can act as pump and probe laser and prepare different charge-transfer states within the neutral ferrocene, we expected a difference between the pulse sequence resulting in an asymmetric transient peak. But no evidence for an asymmetric peak was found. The solid lines are theoretical results fitted to the experimental curves. They will be described in section C.

Figure 7 shows similar results for the dynamic behavior at different excitation energies of 42 195 cm^{-1} ($\lambda_{pu} = 237$ nm) and 37 735 cm^{-1} ($\lambda_{pr} = 257$ nm). Both are assigned to a transition within the Cp ring. The laser pulses with a wavelength of 237 nm are the pump pulses in this experiment according to our definition given above. Basically no differences from the results in Figure 6 are seen. There is only a slight difference between the transients at longer delay times in Figures 6 and 7. In the latter the ion signal measured at the mass of ferrocene has the same value for positive as well as for negative delay times. Only the signal measured at the mass of FeCp$^+$ shows a small increase of the signal at positive delay similar to that in Figure 6. This can be explained by different absorption coefficients and laser pulse intensities. The short time dynamics is not different for the chosen wavelengths. From the experimental results in Figures 6 and 7 we see that the dissociation dynamics (<1 ps) of neutral electronical excited ferrocene does not depend on the excitation energy between 36 750 and 42 200 cm^{-1}.

2. Fe$^+$ from Ionic and Neutral Dissociation? There are two mechanisms possible for the productions of Fe$^+$ after photo-excitation of ferrocene: (i) Fe originates from a dissociation in the intermediate electronically excited state of ferrocene (neutral channel) and is then ionized by absorption of two photons from the probe pulse: An increase of the Fe$^+$ signal is expected for a delay of the probe pulse by the typical lifetime of the intermediate state if neutral Fe is produced instantaneously after the decay of the intermediate state of ferrocene. This means that no long-lived intermediate is produced after dissociation of ferrocene. (ii) Production of Fe$^+$ in a fragmentation process of excited (≈ 7 eV internal energy) ferrocene cations after three-photon absorption.

In Figure 8 the transient pump$-$probe signal of the ion current

Dissociation Dynamics of Ferrocene

J. Phys. Chem. A, Vol. 105, No. 23, 2001 **5581**

Figure 8. Two-color subpicosecond transient signal measured at the mass of the fragment ion Fe^+ of ferrocene for a pump pulse wavelength of 237 nm and a probe pulse wavelength of 257 nm. The solid line represents the best fit of the calculation (for details, see text).

at 56 u, the mass of Fe^+, is shown for the pump excitation energies of 42 195 cm^{-1} (λ_{pu} = 237 nm) and the probe energy of 37 735 cm^{-1} (λ_{pr} = 257 nm). The signal was recorded simultaneously with the $Fe(Cp)_2^+$ and $FeCp^+$ signal shown in Figure 7. There is only a small sub-picosecond transient located on the constant background. It has about the same width as the ferrocene ion $Fe(Cp)_2^+$ and $Fe(Cp)^+$ ion signals in Figure 7. Within the experimental accuracy the rising time of this peak coincides with that of the $Fe(Cp)^+$ ion signal and shows no indication for a delay as would be expected for the production from a neutral dissociation channel (i). This points to the ionic channel (ii) as mainly responsible for the Fe^+.

This result from pump–probe time-resolved experiments corroborates our recent conclusion from the intensity dependence and the observed mass pattern in our femtosecond mass spectroscopy experiments.[34] We cannot completely exclude that there exist contributions from the neutral dissociation channel (i) because of the noisy signal in Figure 8.

3. Bridged Ferrocene Ion. The influence of a bridge between the Cp rings on the fast dissociation process in the intermediate state is investigated by means of the dynamics behavior measured for the ferrocene derivative [3]-ferrocenophan (Figure 1b). As discussed above, the bridge has no influence on the dissociation behavior after nanosecond laser excitation and only Fe^+ ions were detected as for unbridged ferrocene. $FeCp^+$ is the main fragment in the femtosecond mass spectrum of ferrocene, but we did not find it in the femtosecond mass spectrum of [3]-ferrocenophan. From this we conclude that the bridge leads to a stabilization in the ionic [3]-ferrocenophan. The transient signals of the parent cation [3]-ferrocenophan (226 u, lower trace) and the resulting Fe^+ (56 u, upper trace) are shown in Figure 9 for a laser wavelengths of 244 and 272 nm. Since in the case of [3]-ferrocenophan no data are available on electronic transitions energies, the wavelengths were chosen as in the case of ferrocene. The ion signal of the [3]-ferrocenophan parent cation shows the same constant signal level baseline for long positive and negative delay times. The subpicosecond transient dynamics is the same as for ferrocene, discussed above. In addition, the Fe^+ signal in the upper trace of Figure 9 shows a similar temporal behavior as in the case of ferrocene (Figure 8), where we concluded that Fe^+ results from the ionic fragmentation of the ferrocene cation (ionic channel). Furthermore we find a small delay of the peak maxima in the Fe^+ and the $Fe(C_5H_4)_2C_3H_6^+$ signals similar to the delay between ferrocene and the ferrocene fragment $FeCp^+$.

C. Discussion. *1. Model.* We describe the dynamics of the femtosecond excitation and dissociation of ferrocene in the
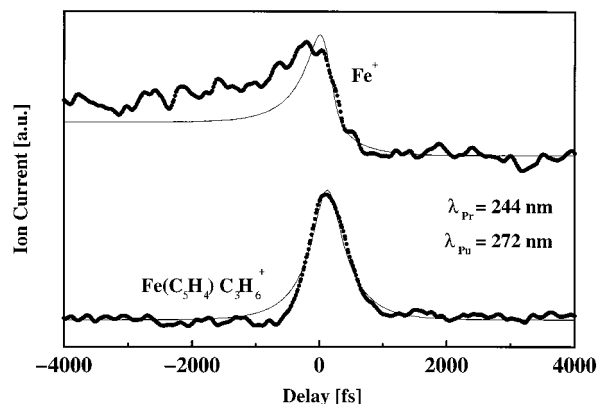
Figure 9. Two-color subpicosecond transients measured at the mass of the [3]-ferrocenophan cation (lower trace) and its fragment ion Fe^+ for a pump pulse wavelength of 244 nm and a probe pulse wavelength of 272 nm. The two traces have different zero levels and vertical scales (see peak heights peak heights in Figure 5). The solid line represents the best fit of the calculation (for details, see text).
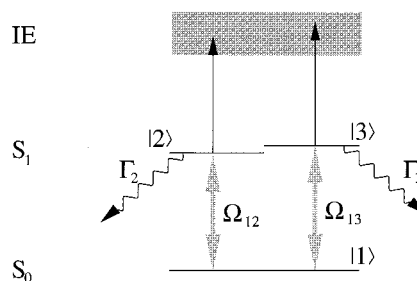
Figure 10. Energy level scheme of the pump–probe experiment of this work. Level $|1\rangle$ represents the ground state of ferrocene, which is coherently coupled to the excited states $|2\rangle$ and $|3\rangle$ by two strong resonant laser fields of different wavelengths. Both laser pulses can ionize the system (shaded area) in an incoherent excitation step from the intermediate states $|2\rangle$ and $|3\rangle$. Ω_{12} and Ω_{13} are the Rabi frequencies of the transition $|2\rangle \leftarrow |1\rangle$ and $|3\rangle \leftarrow |1\rangle$, which are excited by the pump and probe pulses. Γ_2 and Γ_3 are the decay rates of the respective levels.

intermediate electronically excited state of the ferrocene by the schematic energy level scheme shown in Figure 10. Ferrocene is excited by single-photon absorption either from the pump or the probe laser pulse to rapidly decaying excited states $|2\rangle$ and $|3\rangle$. The origin for the rapid decay is, e.g., a repulsive potential energy surface[12,13] or a conversion of electronic to vibrational energy.[11] The fast dissociation is described by two phenomenological decay rates Γ_2 and Γ_3 of level $|2\rangle$ and $|3\rangle$, respectively. From state $|2\rangle$ and $|3\rangle$ further photons can be absorbed to the ionization continuum, marked by the shaded area in Figure 10. The time evolution of states $|2\rangle$ and $|3\rangle$ is probed by a second delayed femtosecond laser pulse. The two levels $|2\rangle$ and $|3\rangle$ shown in Figure 10 take into account the dense electronic state manifold in ferrocene. Photons from both the pump and the probe pulse can be absorbed in the first step, even if the pump and the probe pulse differ in their wavelength. There are only small differences in the mass spectra for femtosecond pulses with wavelengths between 272 and 236 nm. Thus it is clear that an interpretation of the measured transients is complicated because each laser pulse can act as the pump or the probe pulse, respectively.

For a solution of the three-level system coupled by a resonant light field (Figure 10) we used the rotating wave approximation.[42,43] Recently, this model together with a numerical solution was successfully applied to the coherent ion dip spectroscopy of polyatomic molecules in our group.[44–46] The ground level is

coupled by two laser pulses of different wavelengths to two different intermediate states. We assume that the laser pulse frequencies are in resonance with these intermediate states. The energy levels $|2\rangle$ and $|3\rangle$ have different decay rates Γ_i ($i = 2$, 3).

Both laser pulses can ionize the molecule by absorption of an addition photon in the intermediate states. Assuming a constant absorption rate into the ionization continuum, the second absorption step can be described by a time-dependent decay rate $\Gamma(t)^{\text{ion}}$. Because of the very fast ionization process, $\Gamma(t)^{\text{ion}}$ follows the shape of the laser pulses represented by a Gaussian shape $f_{\lambda i}(t)$ with i equal to 1 or 2 for the two laser pulses (eq 3). This means that coherence effects can be excluded and a population which has reached the ionic state cannot recur to the intermediate state.

The three-level system is described by three coupled linear differential equations, where the probability amplitudes c_i ($i = 1-3$) are complex numbers:

$$\frac{2}{i}\frac{d}{dt}\begin{pmatrix} c_1(t) \\ c_2(t) \\ c_3(t) \end{pmatrix} = \begin{pmatrix} 0 & \Omega_{12} & \Omega_{13} \\ \Omega_{12} & i\Gamma_2(t) & 0 \\ \Omega_{13} & 0 & i\Gamma_3(t) \end{pmatrix}\begin{pmatrix} c_1(t) \\ c_2(t) \\ c_3(t) \end{pmatrix} \qquad (1)$$

with

$$\Gamma_i(t) = \Gamma(t)^{\text{ion}} + \Gamma_i^{\text{decay}}, \quad i = 2, 3 \qquad (2)$$

and

$$\Gamma(t)^{\text{ion}} = \Gamma_{\lambda 1}^{\text{ion}} f_{\lambda 1}(t) + \Gamma_{\lambda 2}^{\text{ion}} f_{\lambda 2}(t) \qquad (3)$$

$$\Omega_{kl} = \frac{1}{\hbar}\vec{\mu}_{kl}\vec{\epsilon}\, f_{\lambda i}(t) = \Omega_{lk} \qquad (4)$$

The coupling between the different levels is described by the Rabi frequency Ω_{kl}, which is proportional to the transition strength in the dipole approximation for the light field ($\vec{\mu}_{kl}\vec{\epsilon}$) and the laser pulses (eq 4).

The decay rate $\Gamma_i(t)$ is the sum of the decay rate of a single intermediate state (Γ_i^{decay}, $i = 2$ *or* 3) and the population decay caused by the ionization process and represented by a time dependent decay rate $\Gamma(t)^{\text{ion}} = \Gamma_{\lambda 1}^{\text{ion}} f_{\lambda 1}(t) + \Gamma_{\lambda 2}^{\text{ion}} f_{\lambda 2}(t)$ of the two laser pulses (see above).

The population of the different levels is given by the norm of the probability amplitude:

$$P_k(t) = |c_k(t)|^2, \quad k = 1, 2, 3 \qquad (5)$$

In our experiment we measured the ion current, which is proportional to the population in the ionic state. Its calculation is possible, as well as that of the concentration of a possible neutral dissociation product caused by the finite lifetime of the intermediate states. The system of three coupled differential equations is solved numerically with a Runge Kutte procedure.[47]

2. Only One Laser Pulse Causes Dissociation. First we applied the model calculations to the three-level system and an usual pump−probe scheme, where only the pump pulse can excite the molecules to an intermediate state with a pulse duration of 200 fs. The coupling between ground state (level $|1\rangle$) and the two intermediate states (level $|2\rangle$ and $|3\rangle$) is weak and represented by the Rabi frequencies Ω_{12} and Ω_{13}. The lifetime of the level $|2\rangle$ is chosen to 10 fs which is very short and therefore describes a nonresonant transition. Γ_3^{-1} of level $|3\rangle$ represents the dissociation time of a real intermediate level and is varied between 10 fs and 10 ps. Both laser pulses can
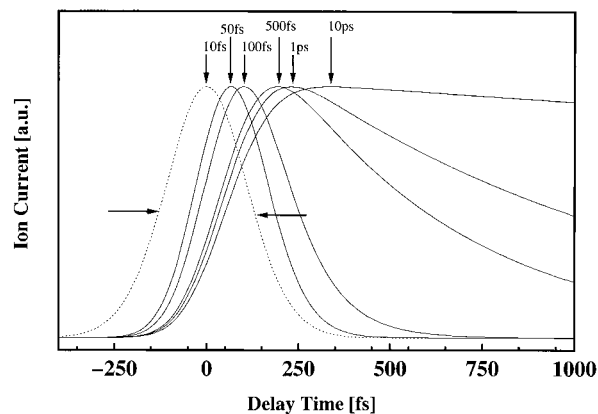

Figure 11. Ion signal calculated for the level scheme in Figure 10 as a function of the delay time between the pump and the probe pulse with a pulse length of 200 fs. The lifetime of the intermediate state $|2\rangle$ is taken as 10 fs, representing a nonresonant excitation. The lifetime of the second intermediate state $|3\rangle$ is varied between 10 fs and 10 ps. For a very short lifetime (10 fs) of the intermediate state $|3\rangle$ the calculated transient represents the crosscorrelation of the laser pulses (dashed line). With increasing lifetime of level $|3\rangle$ the transient peak maximum is shifted to longer delay times and the peak width is increasing. If the lifetime of the intermediate state is much longer than the laser pulse duration an exponential decay is found.

ionize the system very effectively which is represented by a high decay rate $\Gamma(t)^{\text{ion}}$. In Figure 11 the normalized calculated results for the ion current are shown for different lifetimes of level $|3\rangle$ of 10, 50, 100, 500, 1, and 10 ps. For times much shorter than the pulse length, the time behavior of the ion current is given by the crosscorrelation of the pump and probe laser pulses (see also Figure 3). For a pulse length comparable to the dissociation time of level $|3\rangle$, a more complicated dynamic behavior is observed with a peak maximum shifted toward longer delay times with increasing lifetime of level $|3\rangle$ and the peak width increasing simultaneously. If the lifetime of the intermediate state is much longer than the pulse duration, the ion current shows an exponential decay behavior. The result in Figure 11 allows one to determine dissociation lifetimes which are shorter or in the range of the laser pulse. However, we would like to emphasize again that this simple situation is not realized in ferrocene, since both pump and probe laser pulses lead to a population in the intermediate state. Similar approaches were made by Freudenberg et al.[48] They did not solve the Schrödinger equation for a three-level system in the rotating wave approximation numerically but used the optical Bloch equations in the rotating wave approximation to deduce decay times in several systems (see ref 49 and references therein).

For higher coupling strength between two energetic levels, the population of the ground and the excited state shows typical Rabi oscillations and the dissociation product, e.g., the neutral Fe has a steplike increase. The calculated result is demonstrated in Figure 12 for a two-level system where level $|1\rangle$ (i.e., the ground state) and $|2\rangle$ (i.e., a dissociating excited state) are strongly coupled by a laser field. The lifetime of state $|2\rangle$ is fixed to 250 fs, and the laser pulse width is 200 fs (fwhm). Obviously, this situation is not realized in our experiment and no oscillations are observed in the experimental curves in Figures 6−9.

3. Both Laser Pulses Cause Dissociation. If the absorption of both the pump and probe laser pulses with different wavelengths leads to a dissociation, the conventional pump−probe scheme with a pump pulse preparing the system and a second laser pulse probing it fails. For ferrocene we have to consider the dissociation after excitation with both UV laser

Dissociation Dynamics of Ferrocene

J. Phys. Chem. A, Vol. 105, No. 23, 2001 **5583**
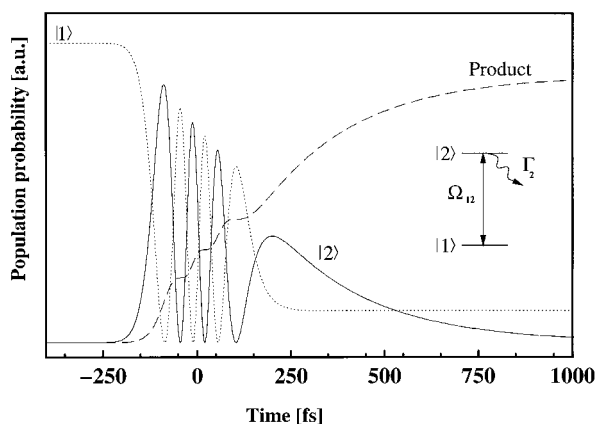
Figure 12. Calculated population dynamics of the two levels $|1\rangle$ and $|2\rangle$ strongly coupled by a laser field. Inset: Scheme of the coupled two level. The lifetime of state $|2\rangle$ is given by a fast dissociation process and fixed to 250 fs, and the laser pulse width is 200 fs (fwhm). The population is oscillating between both states with the Rabi frequency Ω_{12}. The population of the dissociation product (dashed line) is steplike increasing.
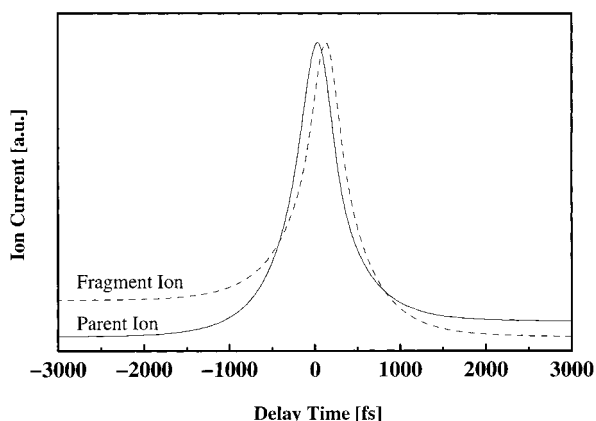

Figure 13. Calculated signal of the parent ion after excitation according to the level scheme in Figure 10. Fragment ion current originating from a fragmentation of the parent ion after further photon absorption. Note, that the maximum of the fragment ion signal is delayed from the parent ion maximum.

pulses. This means that both UV pulses can act as pump and probe pulse. The efficiency for the different excitation and fragmentation steps within the ion might be different for the two pulses. In such a case the measured decay of the signal, e.g., the ion current, cannot be directly taken as the decay of the involved intermediate states.

If the intermediate states have a lifetime smaller than or in the range of the laser pulse lengths, the population of the ground state is pumped very efficiently to the ionic state during the overlap time of the laser pulses. Obviously, the intermediate state is bypassed; i.e., the dissociation in the neutral intermediate state is of minor importance and the signal of the neutral dissociation product decreases at zero delay time, leading to a dip in the signal. This behavior is confirmed by the model calculations.

A further absorption of photons within the ferrocene *cations* can be taken into account by extension of the model shown above in a rate equation approximation. The calculated signal of the ionic fragment channels shows a delay of their transient peak maxima from that of the parent ion signal. Furthermore, a different constant signal level is observed for longer delay times (see Figure 13), depending on the fragmentation efficiencies in the ion. In a simple picture there is a time delay of the
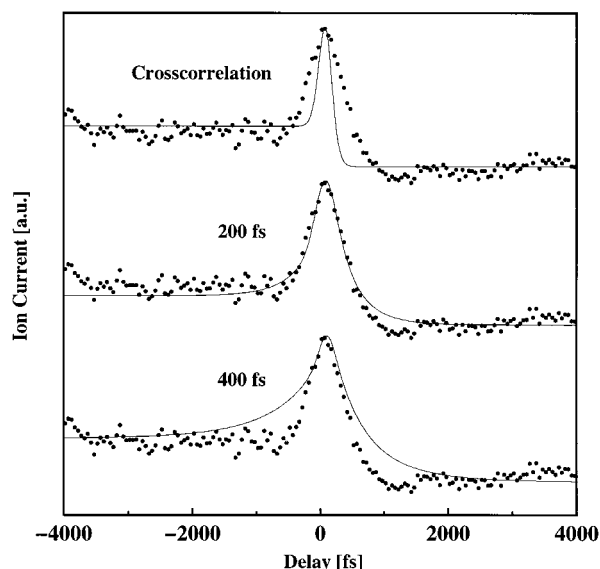
Figure 14. Experimental transient from Figure 6 measured at 186 u (parent signal) compared with three calculated transients with differing intermediate state lifetimes. Top: Intermediate state "lifetime" of 10 fs. The solid line corresponds to the crosscorrelation of the pump and probe pulses. Middle: Intermediate state lifetime of 200 fs. Bottom: Intermediate state lifetime of 400 fs.

fragment ion signal because a sufficient population of the ferrocene cation has to be produced before an effective fragmentation can occur. The signal offset at longer delay times depends on the laser pulse sequence.

We want to point out that a delay between the parent cation and the fragment ion signal as observed in our experiment is only present if further absorption of photons within the parent ion is leading to ionic *fragmentation*. This is different from recent pump–probe experiments of the organometallic molecule $Fe(CO)_5$ of Gerber and co-workers[3] where the pump pulse did not act as a probe pulse and vice versa. These authors interpreted the measured time delay in terms of a dissociation time within the intermediate state of the *neutral* molecule. In our experiment, where both laser pulses could cause neutral dissociation, the ion signal of the dissociation product would show a dip during the laser pulses for a neutral dissociation process (see above) which is not observed.

4. Application to Ferrocene. The calculated results for the subpicosecond transients of the ferrocene cation $Fe(Cp)_2^+$ and its fragment $Fe(Cp)^+$ are given by the solid lines in Figure 6. In the calculation, the lifetimes of the two involved neutral intermediate states $|2\rangle$ and $|3\rangle$ are assumed to be identical. This is a reasonable assumption as both laser pulse frequencies do not differ very much and they have a broad frequency width resulting in a nonselective excitation. Best agreement of experimental results and measured transients was achieved for a lifetime of the intermediate states of about 200 fs. To illustrate this, we compare the time dependence of the pump–probe ion signal at 186 u (ferrocene cation) with three different calculated transients in Figure 14 (see also Figure 6). The solid line in the upper trace represents the crosscorrelation of the laser pulses, with an assumed "lifetime" of the intermediate states of 10 fs. In the middle trace the lifetime was chosen to 200 fs and in the lower trace to 400 fs. The theoretical result for a dissociation time of 200 fs fits best to the experimental data (middle trace) and there is a clear difference from results with very short (10 fs) and longer (400 fs) dissociation time. It is clear that our model can explain the measured time delay between the two ion signal maxima and the different constant signal levels for

longer delay times. At zero delay time, i.e., for overlapping pump and probe laser pulses, no dip is detected. This is in agreement with our conclusions that $FeCp^+$ is produced by a fragmentation of the highly excited ferrocene cation. No clear indications of oscillatory behavior of the transient signal are seen in the experimental curves. We conclude that a sufficiently accurate theoretical description of the present experiment would be possible within a simple rate equation model neglecting coherent effects. Experiments with increased time resolution and higher intensity are planned for the near future to detect the coherent effects. Furthermore, for other ferrocene derivatives with longer decay times and increasing absorption strength, oscillatory behavior of the transients might be expected even for the used 200-fs pulses.

In Figure 7 the measured transients are shown for a pump pulse wavelength of 237 nm and the probe pulse wavelength of 257 nm. Best fit to the experimental curves was achieved for the same lifetime of the intermediate state of 200 fs as in Figure 6. In addition, the subpicosecond transient dynamics induced by pulses at 237/257 nm can be explained by absorption coefficients similar to the ones for the pulses at 244/272 nm shown in Figure 6. There is only a slight difference in the constant background level signals for longer delay times.

The simulation of the observed Fe^+ transients does not show a dip for overlapping laser pulses (see Figure 8). From this, we concluded that the observed Fe^+ ion signal, as in the case of the $FeCp^+$, is mainly given by an *ionic* fragmentation of the ferrocene cation. The subpicosecond dynamics can be reasonably well explained by model calculations using the same parameters as for the $FeCp^+$ transient (solid line in Figure 8). In addition, the neutral channel, i.e., the production of neutral Fe from a dissociation of neutral excited ferrocene and a subsequent ionization, is certainly active in this experiment, but we were not able to clearly identify it. It is possible that this mechanism leads to a constant background in the transients which is hard to detect. Thus only the transient resulting from Fe^+ production by a fragmentation of the ferrocene cation is detected as the dominating signal.

The peak width of the subpicosecond transient of the [3]-ferrocenophan cation shows the same behavior as for ferrocene. Therefore the same decay time of the neutral intermediate state of 200 fs leads to the solid line in the lower part of Figure 9. The observed Fe^+ transient shows a similar temporal behavior as found for the Fe^+ signal obtained from ferrocene. As discussed above, a constant Fe^+ signal could also originate from the dissociation of neutral excited [3]-ferrocenophan, leading to the production of neutral Fe which is ionized by resonance-enhanced two-photon absorption. This mechanism is active but is not responsible for the measured Fe^+ transients, showing the typical behavior expected for a production of Fe^+ ions by fragmentation of the [3]-ferrocenophan cation. From the same lifetime of the neutral excited state of ferrocene and [3]-ferrocenophan, we conclude that there is no stabilization of the bridge in the neutral excited intermediate state, which would lead to a longer lifetime. Most likely the observed lifetime is given by the dissociation of ferrocene leading to neutral Fe. This may be concluded from the nanosecond mass spectra, where the production of neutral Fe is the dominating process for neutral excited ferrocene as well as for [3]-ferrocenophan. The same lifetime of the neutral excited intermediate state of ferrocene and [3]-ferrocenophan points to a fast dissociation process with a concerted breaking of all metal–ligand bonds and a production of Fe within 200

fs. Future experiments will include the investigation of the dissociation dynamics of multiple bridged ferrocenes to check this model.

IV. Summary

In this work we present pump–probe experiments of ferrocene and [3]-ferrocenophan with 200-fs UV pulses. Parent ions are produced by absorption of two UV photons. The absorption of further photons within the parent ion leads to an ion internal energy high enough to open different ionic fragmentation channels.

The application of UV pump and probe pulses results in a special situation differing from recent pump–probe experiments of metal carbonyls,[3,4] where only the pump pulse causes dissociation in the neutral molecule. Because of the broad absorption bands of ferrocene in the investigated spectral range, each laser pulse can act as a pump– and probe–pulse at the same time. We describe the experiment with a theoretical model taking into account this ambiguity. In particular, it includes a neutral dissociation channel and ionic fragmentation channels. The coupling between the ground state and two intermediate states is described in the rotating wave approximation of the Schrödinger equation of a three-level system. Ionization of the excited system is taken into account by a time-dependent decay rate leading to the production of ferrocene cations. We consider the further absorption of photons within the parent cation in a rate equation approach.

The measured dynamic behavior of the transients of different ion signals allows us to distinguish a neutral dissociation from a fragmentation of the parent cation. From the transients of the *parent cation* produced by two-photon absorption, the dissociation time of the intermediate state is found. The measured time dependence of the parent ion signal is theoretically reproduced best for a decay time of the excited neutral level of 200 fs. From the measured *fragment ion* transients $FeCp^+$ and Fe^+ and a comparison with theoretical calculations we conclude that they are produced by an ionic channel, i.e., the fragmentation of the parent cation. A contribution of the neutral channel to the Fe^+ signal is present but cannot be clearly analyzed. This supports our recent conclusions from mass spectra measured with fs pulses.[34] The measured dissociation dynamics does not depend on the nature of the excited charge transfer state (metal-to-ligand, ligand-to-metal transition, and transition within the Cp ring).

For the bridged derivative of ferrocene ([3]-ferrocenophan) we found the same dynamic behavior with a lifetime of the neutral intermediate states of 200 fs. This is an indication for a dissociation mechanism in the neutral intermediate state that is not influenced by the bridge between the two Cp rings, e.g., if all metal–ligand bonds break in a concerted dissociation process and neutral Fe is produced within 200 fs.

References and Notes

(1) Zewail, A. H. *Femtochemistry: Ultrafast dynamics of the chemical bond;* World Scientific: Singapore, 1994.

Dissociation Dynamics of Ferrocene

J. Phys. Chem. A, Vol. 105, No. 23, 2001 **5585**

(2) Bergt, M.; Kiefer, B.; Gerber, G. *J. Mol. Struct.* **1998**, *207*, 480−481.

(3) Banares, L.; Baumert, T.; Bergt, M.; Kiefer, B.; Gerber, G. *J. Chem. Phys.* **1998**, *108*, 5799.

(4) Kim, S. K.; Pedersen, S.; Zewail, A. H. *Chem. Phys. Lett.* **1995**, *233*, 500.

(5) Kealey, T. J.; Pauson, P. L. *Nature* **1951**, *168*, 1039.

(6) Togni, A.; Hayashi, T. *Ferrocenes;* VCH: Weinheim, New York, 1995.

(7) Armstrong, A. T.; Smith, F.; Elder, E.; McGlynn, S. P. *J. Chem. Phys.* **1967**, *46*, 4321.

(8) Leutwyler, S.; Even, U.; Jortner, J. *J. Phys. Chem.* **1981**, *85*, 3026.

(9) Leutwyler, S.; Even, U.; Jortner, J. *Chem. Phys. Lett.* **1980**, *74*, 11.

(10) Engelking, P. C. *Chem. Phys. Lett.* **1980**, *74*, 207.

(11) Nagano, Y.; Achiba, Y.; Kimura, *J. Phys. Chem.* **1986**, *90*, 1288.

(12) Liou, H. T.; Ono, Y.; Engelking, P. C.; Moseley, J. T. *J. Phys. Chem.* **1986**, *90*, 2888.

(13) Liou, H. T.; Engelking, P. C.; Ono, Y.; Moseley, J. T. *J. Phys. Chem.* **1986**, *90*, 2892.

(14) Ray, U.; Hui, H. Q.; Zhang, Z.; Schwarz, W.; Vernon, M. *J. Chem. Phys.* **1989**, *90*, 4248.

(15) Opitz, J.; Härter, P. *Int. J. Mass. Spectrom. Ion. Proc.* **1992**, *121*, 183.

(16) Lewis, K. E.; Smith, G. P. *J. Am. Chem. Soc.* **1984**, *106*, 4650.

(17) Connor, J. A. *Top. Curr. Chem.* **1977**, *71*, 71.

(18) Wilkinson, G.; Pauson, P. L.; Cotton, F. A. *J. Am. Chem. Soc.* **1954**, *76*, 1970.

(19) Han, S.-J.; Yang, M. C.; Hwang, C. H.; Woo, D. H.; Hahn, J. R.; Kang, H.; Chung, Y. *Int. J. Mass. Spectrom.* **1998**, *181*, 59.

(20) Bär, R.; Heinis, Th.; Nager, Ch.; Jungen, M. *Chem. Phys. Lett.* **1982**, *91*, 440.

(21) Barfuss, S.; Emerich, K.-H.; Hirschwald, W.; Dowben, P. A.; Boag, N. M. *J. Org. Chem.* **1990**, *391*, 209.

(22) Begun, G. M.; Compton, R. N. *J. Chem. Phys.* **1973**, *58*, 2271.

(23) Flesch, G. D.; Junk, G. A.; Svec, H. J. *J. Chem. Soc. Dalton Trans.* **1972**, *11*, 1102.

(24) Puttemans, J.-P.; Hanson, A. *Ing. Chim.* **1971**, *53*, 17.

(25) Muller, J.; D'Or, L. *J. Organomet. Chem.* **1967**, *10*, 313.

(26) Ryan, M. F.; Eyler, J. R.; Richardson, D. E. *J. Am. Chem. Soc.* **1992**, *114*, 8611.

(27) Rabalais, J. W.; Werme, L. O.; Bergmark, T.; Karlsson, L.; Hussain, M.; Siegbahn, K. *J. Chem. Phys.* **1972**, *57*, 1185.

(28) Adamchuk, V. K.; Dmitriev, A. B.; Prudnikova, G. V.; Sorokin, L. S. *Opt. Spectrosc.* **1972**, *33*, 191.

(29) Huttner, G.; Fischer, E. O. *J. Organomet. Chem.* **1967**, *8*, 299.

(30) Foffani, A.; Pignataro, S.; Distefano, G.; Innorta, G. *J. Organomet. Chem.* **1967**, *7*, 473.

(31) Cauletti, C.; Green, J. C.; Kelly, M. R.; Powell, P.; van Tilborg, J.; Robbins, J.; Smart, J. *Electron Spectrosc. Relat. Phenom.* **1980**, *19*, 327.

(32) Evans, S.; Green, M. L. H.; Jewitt, B.; Orchard, A. F.; Pygall, C. F. *J. Chem Soc. Faraday Trans.* **1972**, *68*, 1847.

(33) Evans, S. H.; Green, M. L.; Jewitt, B.; King, G. H.; Orchard, A. F. *J. Chem. Soc., Faraday Trans.* **1974**, *70*, 356.

(34) Clara, M.; Braun, J. E.; Hellerer, Th.; Neusser, H. J. *Int. J. Mass Spectrom. Ion Proc.* **2000**, *203*, 71.

(35) Grun, C.; Weickhardt, C.; Grotemeyer, J. *Eur. Mass Spectrom.* **1996**, *2*, 197.

(36) Weickhardt, C.; Moritz, F.; Grotemeyer, J. *Eur. Mass Spectrom.* **1996**, *2*, 151.

(37) Clara, M.; Hellerer, Th.; Neusser, H. *J. Appl. Phys. B* **2000**, *71*, 431.

(38) Boesl, U.; Neusser, H. J.; Weinkauf, R.; Schlag, E. W. *J. Phys. Chem.* **1982**, *86*, 4857.

(39) Hellerer, Th. Diplomarbeit, Technische Universität München, 1999.

(40) Rinehard, K. L.; Curby, R. J.; Gustafson, D. H.; Harrison, K. G.; Bozak, R. E.; Bublitz, D. E. *J. Am. Chem. Soc.* **1962**, *84*, 3263.

(41) Braun, J. E.; Neusser, H. J.; Härter, P.; Stöckl, M. *J. Phys. Chem.* **2000**, *104*, 2013.

(42) Cantrell, C. D.; Letokhov, V. S.; Makarov, A. A. In *Coherent Nonlinear Optics;* Feld, M. S., Letokhov, V. S., Eds.; Springer: Berlin, 1980.

(43) Shore, B. W. *The Theory of Coherent Atomic Excitation;* Wiley: New York, 1990.

(44) Neuhauser, R.; Braun, J.; Neusser, H. J.; van der Avoird, A. *J. Chem. Phys.* **1998**, *108*, 8408.

(45) Sumann, R.; Neuhauser, R.; Neusser, H. J. *J. Chem. Phys.* **1995**, *103*, 3315.

(46) Neuhauser, R.; Sussmann, R.; Neusser, H. *J. Phys. Rev. Lett.* **1995**, *74*, 3141.

(47) Press: W. H.; Teukolsky, S. A.; Vetterling, W. T.; Flannery, B. P. *Numerical recipes in C: The art of scientific computing;* Cambridge University Press: Cambridge, 1992.

(48) Freudenberg, Th.; Radloff, W.; Ritze, H.-H.; Stert, V.; Weyers, K.; Noack, F.; Hertel, I. V. Z. *Phys. D.* **1996**, *36*, 349.

(49) Stert, V.; Farmanara, P.; Radloff, W. *J. Chem. Phys.* **2000**, *112*, 4460.